ELSEVIER

Journal of Chromatography A, 688 (1994) 301–316

JOURNAL OF CHROMATOGRAPHY A

Development of a capillary electrophoresis method for the characterization of enzymatic products arising from the carbamoylase digestion of paralytic shellfish poisoning toxins☆

A. Buzy, P. Thibault*, M.V. Laycock

Institute for Marine Biosciences, National Research Council, 1411 Oxford Street, Halifax, Nova Scotia B3H 3Z1, Canada

First received 30 June 1994; revised manuscript received 31 August 1994

Abstract

A sample stacking procedure is presented for the capillary electrophoretic (CE) separation of paralytic shellfish poisoning (PSP) toxins dissolved in high ionic strength buffers. The application of such a stacking procedure prior to the zone electrophoretic separation is demonstrated for the analysis of decarbamoyl toxins arising from the digestion of PSP toxins by an hydrolytic enzyme from little neck clams (*Protothaca staminea*). Improvements in separation efficiency facilitated identification and quantitation of substrates and enzymatic products present in the digest using CE. The separation conditions developed were found to be entirely compatible with electrospray mass spectrometry, which permitted the analysis of PSP toxins and their decarbamoyl derivatives present in the low micromolar range in crude enzyme digests. The products released during the enzymatic digestion were identified using CE combined with tandem mass spectrometry.

1. Introduction

The toxins associated with paralytic shellfish poisoning (PSP) constitute a group of potent marine phycotoxins produced by certain strains of dinoflagellates such as *Alexandrium* spp. [1,2]. Blooms of these dinoflagellates are unpredictable and constitute a serious public health hazard in view of the rapidity with which toxins can accumulate in the filter-feeding shellfish. Consequently, the exploitation and development of coastal shellfish resources and aquaculture can also be severely threatened in areas where such toxic blooms are encountered.

The toxin composition and profile vary considerably between species of toxic dinoflagellates. This feature has been used previously with some success to study the distribution of dinoflagellate species [3]. Toxins produced by the phytoplankton include compounds such as saxitoxin (STX) and neosaxitoxin (NEO), and a complex suite of sulfate and N-sulfonate analogues (Fig. 1). These toxins also vary in terms of their specific toxicities to mammals. The most potent are the carbamate toxins such as STX, NEO and gonyautoxins 1 and 4 ($GTX_{1,4}$), with specific toxicities (with respect to LD_{50} for intraperitoneal injection in mice) ranging from 400 to 550 μg of STX equivalent per μmol. In

* Corresponding author.

☆NRCC No. 38060.

SSDI 0021-9673(94)00850-7

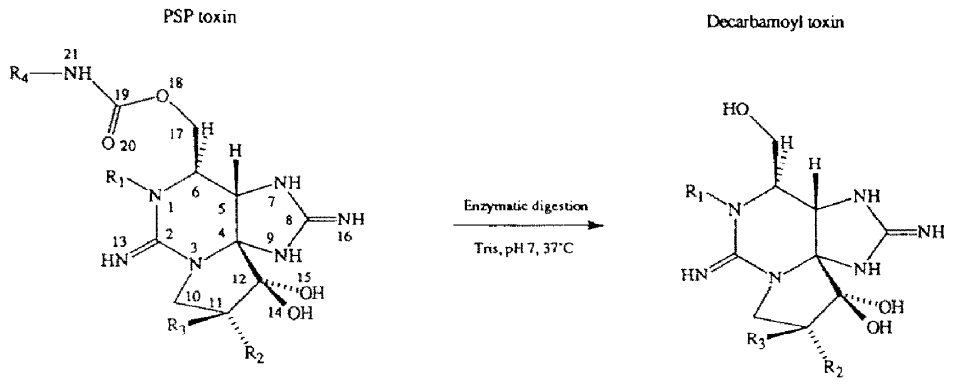

R_1	R_2	R_3	R_4	Toxin	M_r	
H	H	H	H	STX	299	Carbamate toxins
OH	H	H	H	NEO	315	
H	OSO_3H	H	H	GTX_2	395	
H	H	OSO_3H	H	GTX_3	395	
OH	OSO_3H	H	H	GTX_1	411	
OH	H	OSO_3H	H	GTX_4	411	
H	H	H	SO_3H	B_1	379	N-sulfocarbamoyl toxins
OH	H	H	SO_3H	B_2	395	
H	OSO_3H	H	SO_3H	C_1	475	
H	H	OSO_3H	SO_3H	C_2	475	
OH	OSO_3H	H	SO_3H	C_3	491	
OH	H	OSO_3H	SO_3H	C_4	491	

Fig. 1. Paralytic shellfish poisoning toxins: structures, molecular masses and decarbamoyl derivatives.

contrast, the N-sulfocarbamoyl derivatives (B_1, B_2, C_{1-4}) are much less toxic (5–70 μg STXeq./μmol).

The bioaccumulation and transformation of the PSP toxins in shellfish are extremely complex processes. The toxin profiles depend not only on the phytoplankton species on which they have been feeding, but also on the shellfish and the organs examined [4]. In controlled experiments where toxic *Alexandrium* cultures were fed to bivalves, earlier studies have demonstrated that toxin profiles found in a given shellfish species can exhibit significant differences from those of the dinoflagellates [5–9]. Such variations in toxin profiles were found to be species-specific while also displaying a time dependence. Evidence of such variability was also noted in the PSP toxin profiles observed for different populations of wild shellfish species collected from the same geographic location [4,10].

The differences in toxin profiles observed between shellfish and ingested toxic dinoflagellates can be accounted for by a selective retention/elimination of specific toxins and/or by metabolic processes within tissues [4]. One of the stronger pieces of evidence supporting the latter mechanism is the appearance of new toxin components in shellfish that were not present in the original toxic dinoflagellates. Such transformations have been documented for the reduction of

NEO to STX in scallop tissues [11] and for the conversion of $GTX_{1,4}$ to $GTX_{2,3}$ plus STX, and of NEO to STX, by marine bacteria [12]. Although it was originally assumed [11] that such reductions could be mediated enzymatically, recent evidence suggests that these processes could be effected by naturally occurring chemical reductants such as glutathione and cysteine [13]. Formation of de novo toxins was also reported for the conversion of N-sulfocarbamoyl and carbamoyl PSP toxins to their corresponding decarbamoyl derivatives in little neck clams (*Protothaca staminea*) [14] and in two species of Japanese clams [13]. Decarbamoyl toxins have been detected only in a few clam species, and have not been found in most shellfish [13,14].

Evidence accumulated thus far concerning the formation of these decarbamoyl derivatives suggests that loss of the carbamate side chain could be catalysed by hydrolytic enzymes from the bivalve digestive glands. Sullivan et al. [14] indicated that a rapid hydrolysis of PSP toxin substrates (STX, $GTX_{2,3}$, B_1 and $C_{1,2}$) to their corresponding decarbamoyl derivatives (Fig. 1) was observed for homogenates obtained from the viscera of *P. staminea* whereas extracts prepared from the mantle, muscle and siphon yield only limited conversion. An enzymatic process was also indicated by the fact that the conversion was inactivated when the homogenates were exposed to heat, organic solvent (methanol) or low pH [14].

In spite of the numerous studies describing the observation of carbamoylase activity in shellfish, no report has been presented thus far on the isolation and purification of the enzyme(s). This is partly due to the complex nature of the digestive gland extracts and to the lack of a fast, sensitive and efficient chemical-based assay capable of screening fractions obtained during the purification steps. To date, previous studies documenting this specific carbamoylase activity in shellfish extracts have typically used an HPLC–fluorescence detection (FLD) method whereby the separated PSP toxins are converted into fluorescent derivatives using a post-column oxidation procedure [15]. Although this method provides excellent sensitivity (typically 4 ng/ml for STX [15]), the monitoring of carbamoylase activity using this method is difficult in view of the lack of resolution between the substrate and its corresponding decarbamoyl derivative [15]. Improvements in resolution can be achieved using alternate HPLC columns and buffer systems [16], but this is very time consuming since the characterization of all PSP toxins requires a set of three different HPLC conditions, one for each of the toxin groups (STX and NEO, GTXs and C toxins).

In the present study we report the development of a rapid capillary electrophoresis-based method that can be used both for the monitoring of crude enzyme fractions and for the characterization of digestion products. Capillary zone electrophoresis (CZE) with both UV and mass spectral detection has been described previously for the analysis of PSP toxins [17,18]. More recently, enhanced sample loadings for the analysis of PSP toxins was demonstrated using capillary isotachophoresis (cITP) prior to CZE separation [19]. This cITP preconcentration step has provided an improvement of concentration detection limits of at least two orders of magnitude over those obtainable using the conventional CZE format, and facilitated the identification of PSP toxins in biological extracts [19]. This type of sample preconcentration is best effected using coated capillaries to minimize the electroosmotic flow during the cITP step. Unfortunately, the injection of a large number of crude sample extracts can result in irreversible modification of the capillary surface coating, and thus a decrease in the separation performance. Alternate electrophoretic separation procedures capable of handling samples with high salt concentrations or shellfish extracts, with relatively little sample clean-up, were therefore developed for the present application. The judicious choice of electrolyte systems for use with uncoated capillaries enabled proper focusing of the analyte bands even in the presence of highly mobile salts. Mobilization of the PSP toxins was achieved using an acidic buffer, acting as a temporary terminator during the stacking step prior to the zone electrophoresis separation. For purposes of simplicity, the term "capillary electrophoresis"

(CE) will be used here to refer to the combined stacking/zone electrophoresis separation. Such a CE analysis was found to be entirely compatible with the operation of electrospray mass spectrometry (ES-MS), and permitted the monitoring of toxin derivatives formed during the incubation of PSP toxin substrates with crude enzyme extracts from *P. staminea*. Identification and characterization of products released during the enzymatic digestion are demonstrated using on-line CE–ES-MS, and CE with tandem mass spectrometry.

2. Experimental

2.1. Isolation of PSP toxins

Samples of STX, NEO, GTX_{1-4} and $C_{1,2}$ were purified from cultured algal cells of *Alexandrium excavatum* and *A. minutum* according to a procedure described earlier [20]. All toxins were dissolved in 0.1 *M* acetic acid. PSP toxins such as STX, NEO and GTX_{1-4} can also be obtained through the Marine Analytical Chemistry Standards Program (Institute for Marine Biosciences, Halifax, Canada) as individual calibration solutions. The B_1 toxin was obtained following reduction of the $C_{1,2}$ toxins in 0.1 *M* dithiothreitol (Sigma, St. Louis, MO, USA) at 40°C for 1 h. Purification of the reaction products was achieved using a Bio-Gel P-2 column (Bio-Rad Labs., Richmond, CA, USA), eluting the toxin with 0.1 *M* acetic acid [20]. Prior to the enzymatic reaction all PSP standards were dissolved in Tris–HCl to a final buffer concentration of 0.1 *M* and pH 7.

2.2. Preparation of enzyme extracts

Little neck clams (*P. staminea*) were collected from beaches at Bamfield Research Station, Vancouver Island, Canada. All samples were kept frozen at −20°C prior to their extraction. A crude enzyme extract was obtained by dissecting the digestive glands from two clams (5 g wet mass) and grinding in a cold mortar with glass. The homogenized tissues were suspended in 3 ml of 0.1 *M* Tris–HCl, pH 7, and centrifuged at 15 000 *g* for 20 min. The supernatant was concentrated 6 times by ultrafiltration using an Amicon PM-10 membrane (Amicon Canada, Oakville, Canada), and filtered through a 0.22-μm nylon membrane (Millipore, Bedford, MA, USA).

2.3. Toxin incubation

Unless otherwise specified, enzymatic digestions were performed at 37°C using a 40-μl aliquot of PSP toxin solution to which was added 160 μl of the concentrated enzyme extract in Tris buffer pH 7, to give a final toxin concentration between 160 and 240 μg/ml. Aliquots of the reaction mixture (typically 10 μl) were removed at different times, and the digestion process stopped by adding an equal volume of 0.1 *M* HCl. The reaction solution was then neutralized and centrifuged at 10 000 *g* for 5 min to remove those proteins which had precipitated upon the addition of acid. The supernatant was then analyzed directly by CE–UV and CE–MS.

2.4. Capillary electrophoresis

All experiments were performed using a Beckman P/ACE 2100 system (Beckman Instruments, Fullerton, CA, USA). Uncoated fused-silica columns were obtained from Polymicro Technologies (Phoenix, AZ, USA). Unless otherwise specified, dimensions were typically 97 cm (90 cm to UV detector) × 50 μm I.D. × 360 μm O.D. columns. Separations were conducted in constant voltage mode by applying +30 kV at the injector end of the capillary. Samples were introduced by pressurizing the vial with a low (0.5 p.s.i.; 1 p.s.i. = 6894.76 Pa) pressure injection for typically 20 s, resulting in the injection of 20 nl. The CE separation buffer was 100 m*M* morpholine in water adjusted to pH 4.0 with formic acid. Between each run the capillary was washed with 1 *M* NaOH. UV detection was monitored at 200 nm. All concentration measurements were calculated from corrected peak areas (peak area/migration time) to compensate for variation of the electroosmotic flow. All buffer chemicals were purchased from Sigma.

2.5. Mass spectrometer and interface

All MS experiments were performed using a PE/SCIEX API/III$^+$ triple quadrupole mass spectrometer (PE/SCIEX, Thornhill, Canada) equipped with an atmospheric pressure ionization (API) source operated in nebulizer-assisted electrospray (ionspray) mode. The interface was constructed from a fully articulated IonSpray source and is based on a co-axial column arrangement [21] which was subsequently modified in our laboratory [18].

CE–ES-MS analyses used the same CE system as that described above except that the current monitoring function of the Beckman P/ACE 2100 instrument was disabled to permit normal CE operation once the cathodic end of the capillary was connected to the CE–ES-MS interface. In order to minimize the length of the CE column the cartridge was modified so that the capillary exited from the top left corner of the cartridge. Mass spectral acquisition was performed using dwell times of 3 ms per step of 1 u in full mass scan mode, or 100 ms per channel for selected ion monitoring experiments. Fragment ion spectra obtained from combined CE–ES-MS–MS analyses were achieved by selecting the appropriate precursor m/z values in the first quadrupole, and using collisional activation with argon target gas in the high-pressure radio frequency (rf)-only quadrupole collision cell. Collision energies were typically 25 eV in the laboratory-frame of reference, and the collision gas thickness was $3.80 \cdot 10^{15}$ atoms $\cdot$ cm^{-2} deduced from the pressure measured by a Baratron capacitance manometer upstream of the cell. Tandem mass spectra were acquired using dwell times of 3 ms per step of 0.5 u. A MacIntosh Quadra 950 computer was used for instrument control, data acquisition and data processing.

3. Results and discussion

In a series of preliminary experiments different buffer systems were investigated for the analysis of PSP toxin standards. Best separation performance was generally obtained using morpholine at pH 4 in order to minimize the adsorption of PSP toxin on the bare fused-silica surface of the capillary wall, a phenomenon more often observed for NEO and other N^1-hydroxy toxin derivatives. The choice of separation buffer was also motivated by considerations affecting the sensitivity for MS detection. Suitable buffers for CE–ES-MS operation must also carry relatively low currents, be sufficiently volatile to prevent accumulation of residue on the orifice plate, and have low proton affinity to minimize the level of chemical background noise. Amongst the different buffers investigated previously [19] morpholine offered the most accommodating properties.

The separation of PSP toxins on bare fused-silica capillaries was found to be substantially affected by the sample buffer. In particular, the separation performance could not be maintained when the toxins were dissolved in high-ionic-strength buffers such as those used for the enzymatic digestion. An example of this effect is presented in Fig. 2 for the CE–UV analysis of a mixture of the epimeric pair GTX_1 and GTX_4 at a concentration of 360 and 100 μM, respectively, in either 0.1 M acetic acid or Tris buffer at pH 7. When the PSP toxins were prepared in 0.1 M acetic acid, baseline separation of the CE peaks was achieved using a 100 mM morpholine buffer pH 4 on a 57 cm $\times$ 50 μm I.D. capillary (Fig. 2A). Separation efficiencies, calculated from peak widths at half height, were 64 000 and 123 000 theoretical plates for GTX_1 and GTX_4, respectively. The lower number of theoretical plates observed for GTX_1 is due only to the higher concentration of this toxin, and not to adsorption of the toxin on the capillary walls. In the present case, the fact that the sample matrix has a lower conductivity than the running buffer provides an ideal situation for sample stacking. Since a higher field strength will be imparted to the sample zone, ionic analytes will be focused at the boundary of the running buffer. Such stacking conditions also enable the injection of larger sample sizes with minimal zone distortion. Previous studies[19] have demonstrated that using similar electrophoretic systems, sample loadings can be increased to 10% of the capillary volume with negligible degradation of the resolution of the PSP toxins.

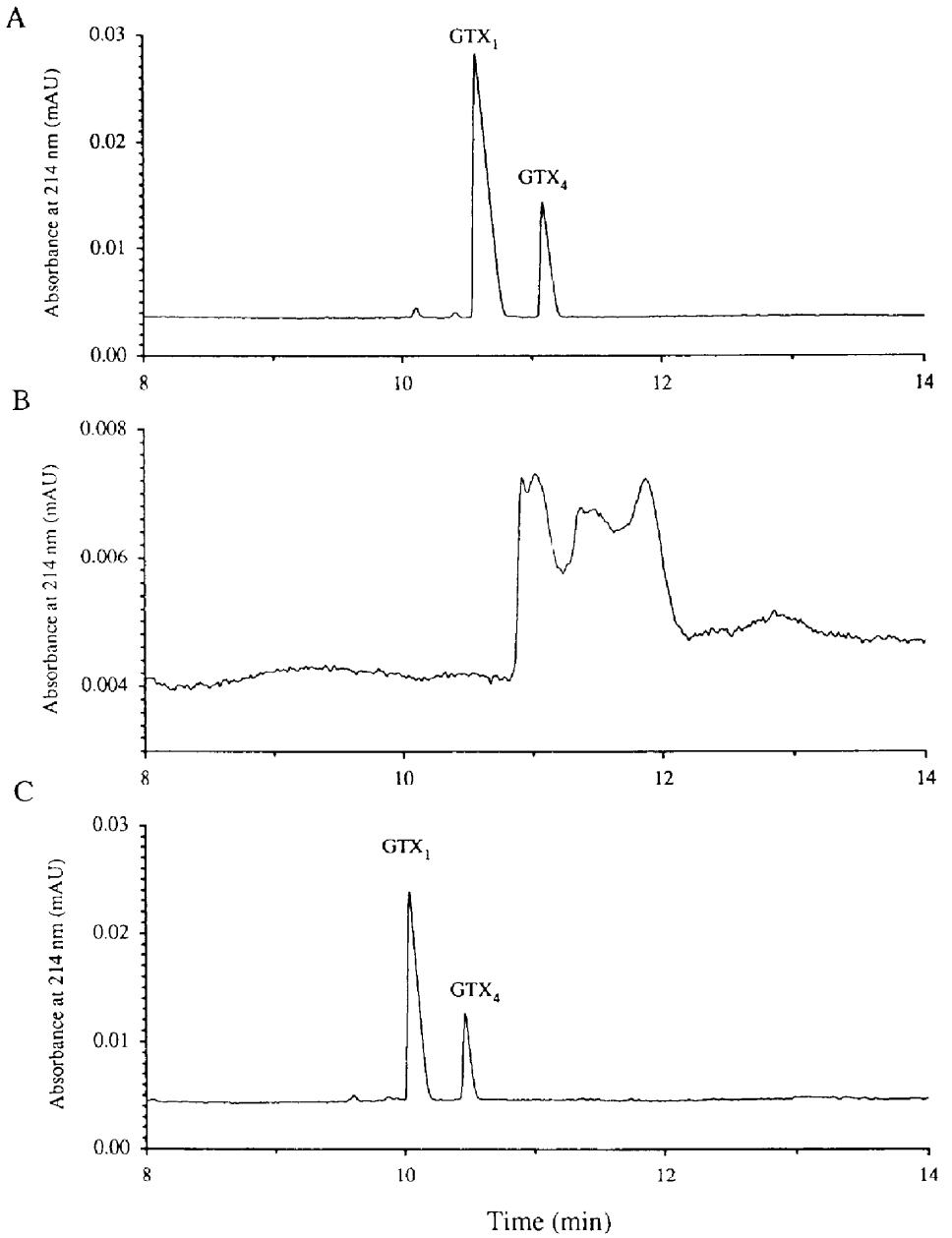

Fig. 2. CE–UV analysis of a mixture of GTX_1 and GTX_4 toxins dissolved in 0.1 *M* acetic acid (A), 50 m*M* Tris pH 7 (B) and 50 m*M* Tris pH 7 with stacking using a terminating electrolyte of 0.1 *M* acetic acid (C). Conditions: 10-nl injection of a standard solution containing GTX_1 (360 μM) and GTX_4 (100 μM), 100 m*M* morpholine pH 4 buffer, bare fused-silica column 57 cm × 50 μm I.D. column for all separations.

In contrast, the CE–UV analysis of the same two toxins dissolved in Tris pH 7 (Fig. 2B) shows very poor separation of GTX_1 and GTX_4, a situation clearly not satisfactory for identification purposes. It is noteworthy that under the same experimental conditions STX and NEO were

resolved (data not shown) owing to their larger electrophoretic mobilities. Sulfated PSP toxins such as GTXs have electrophoretic mobilities ranging from $15 \cdot 10^{-9}$–$17 \cdot 10^{-9}$ m^2 V^{-1} s^{-1} in a morpholine buffer pH 4, whereas the values for STX and NEO are $34 \cdot 10^{-9}$ and $32 \cdot 10^{-9}$ m^2 V^{-1} s^{-1}, respectively.

The difficulty in focusing the GTX toxins is partly attributed to the high conductivity of the Tris sample buffer, and to the low mobilities of these toxins compared to that of the electroosmotic flow ($10 \cdot 10^{-9}$ m^2 V^{-1} s^{-1}, as determined using mesityl oxide). Such conditions are naturally ineffective in providing proper mobilization of the analytes, and lead to anti-stacking effects. In order to alleviate such difficulties, it is possible to focus the sample ions using a discontinuous buffer system in which the separation buffer has a composition different from that of the stacking buffer. The composition of the latter electrolyte is chosen such that it is of a low pH, and possesses a conductivity lower than that of any of the sample or separation buffers. This procedure is similar to that of cITP, except that only 2% of the capillary is filled with the sample and the analyte bands are mobilized in an uncoated capillary with appreciable electroosmotic flow.

Fig. 2C shows the separation of a mixture of GTX_1 and GTX_4 under conditions similar to those used to obtain Fig. 2B, except that a stacking period of 1.5 min using 0.1 *M* acetic acid (pH 3) preceded the zone electrophoresis separation. As observed, resolution of GTX_1 and GTX_4 is now clearly achieved, with separation efficiencies in excess of 100 000 plates for both toxins. The improvement in separation performance is thought to arise from sample stacking where the highly mobile H^+ ions form a temporary leading zone behind the morpholine buffer. Ionic species present in the sample focus into sharp bands behind this leading zone, before the separation is allowed to proceed in a zone electrophoresis format by changing the terminating electrolyte to morpholine.

Separation conditions originally developed with UV detection were also investigated using ES-MS. The CE–ES-MS analyses (20-nl injection) of products released during the enzymatic digestion of a 285 μM solution of NEO, are shown in Fig. 3. In this case, a total of 5 pmol of toxin was injected on the capillary column. The reconstructed ion electropherograms (RIEs) corresponding to the sums of intensities of MH^+ ions of NEO (*m/z* 316) and decarbamoyl (dc)-NEO (*m/z* 273) extracted from the full mass scan acquisition, are presented in Fig. 3A-C for aliquots taken at incubation times of 0, 3 and 6 h, respectively. For purposes of convenience, the analyte signals have been normalized with respect to the intensity of the MH^+ ion of NEO prior to incubation (Fig. 3A). As indicated by the RIE profiles of Fig. 3, the intensity of NEO progressively decreased over the 6-h incubation period. Similarly dc-NEO toxin, which migrates just before NEO, shows a corresponding increase of intensity over the same time period, and is of almost equal abundance to that of NEO at 6 h (Fig. 3C). The identities of the substrate and enzymatic reaction product were confirmed from their full mass spectra, as illustrated in Fig. 4 for the CE peaks migrating at 11.8 and 12.2 min in Fig. 3C. The mass spectra of dc-NEO (Fig. 4A) and NEO (Fig. 4B) both show an abundant ion corresponding to the protonated molecule (MH^+) together with a sodiated adduct (MNa^+).

In a separate series of experiments, the temporal profile of the enzyme digestion of NEO was also monitored by CE–UV detection to ensure that no other product was released during the digestion. Fig. 5 compares the results of the CE–UV analyses with those of CE–ES-MS acquired in selected ion monitoring acquisition mode for *m/z* 273 and 316. In view of the fact that no standard of known concentration was available for dc-NEO, the response factors of this toxin for both UV and ES-MS detection were assumed to be the same as those for NEO. This assumption was justified on the basis that the two guanidino groups of the perhydropurine skeleton are the major chromophores absorbing at 200 nm, and are thus not likely to be affected by substitution taking place on the C-17 side chain. Similarly the same two basic functionalities are the most likely sites of protonation on

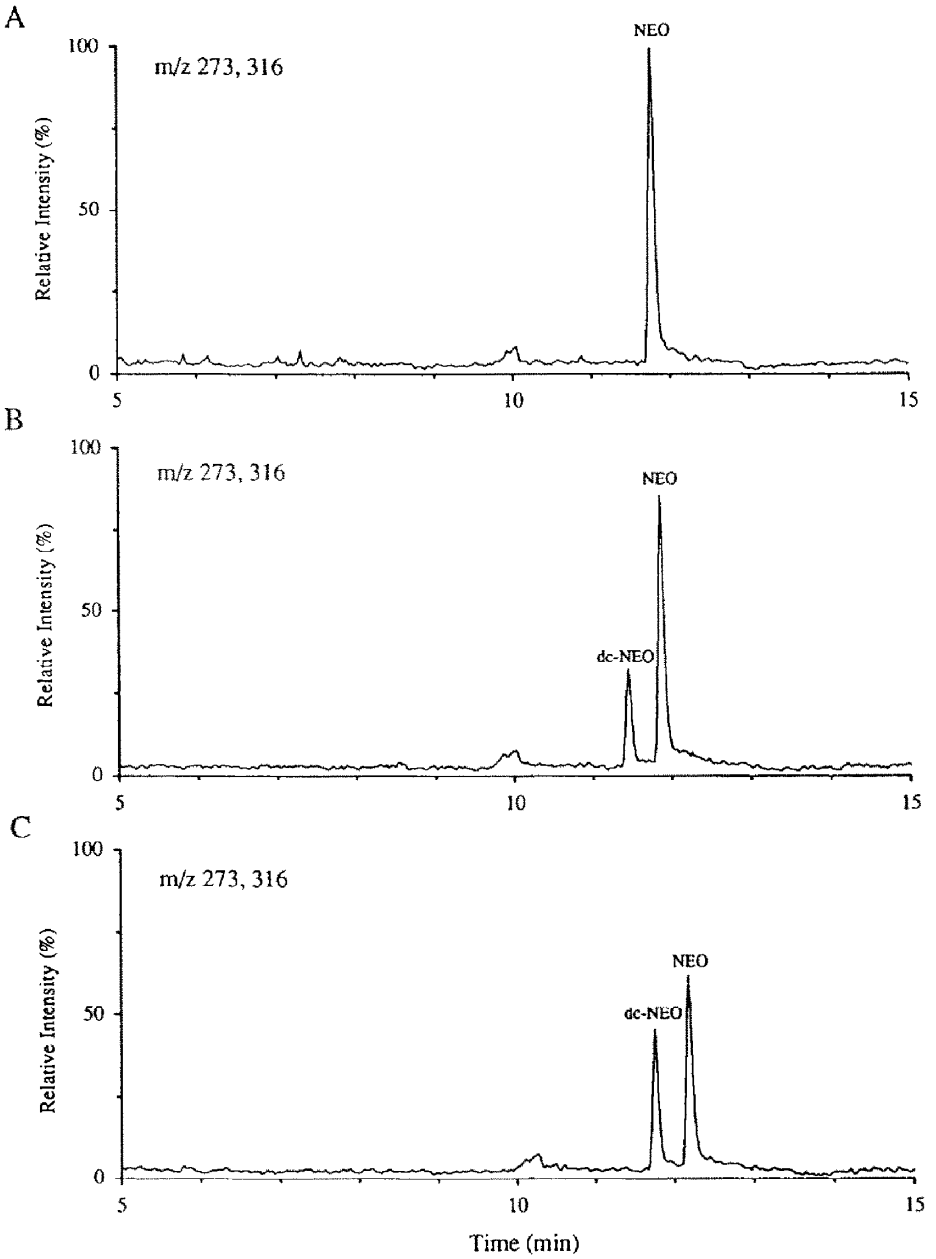

Fig. 3. Reconstructed ion electropherogram for the composite signals at m/z 273 and 316 extracted from the CE–ES-MS analysis (m/z 200–500) of an enzyme digest of NEO toxin. Ion current profiles taken after an incubation period of 0 (A), 3 (B) and 6 h (C). Conditions: 20-nl injection of NEO solution (285 μM) incubated with 140 μl of a crude clam homogenate extract, 35 mM morpholine pH 4 separation buffer, 0.1 M acetic acid terminating electrolyte, bare fused silica column 97 cm × 50 μm I.D. column.

the molecule and electrospray ionization would be therefore expected to yield similar responses for dc-NEO and NEO.

Hydrolysis of NEO to the dc-NEO toxin was found to proceed readily, and a dc-NEO peak corresponding to an intensity of 5% of the

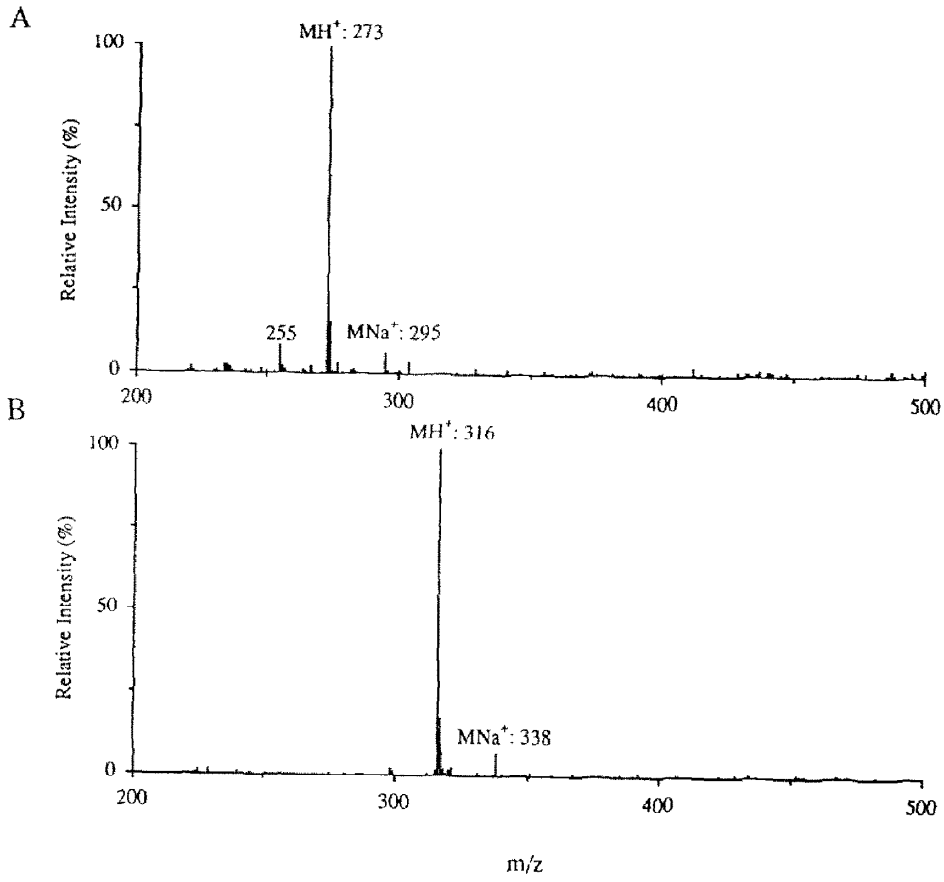

Fig. 4. Extracted mass spectra for peaks migrating at (A) 11.8 and (B) 12.2 min in Fig. 3C.

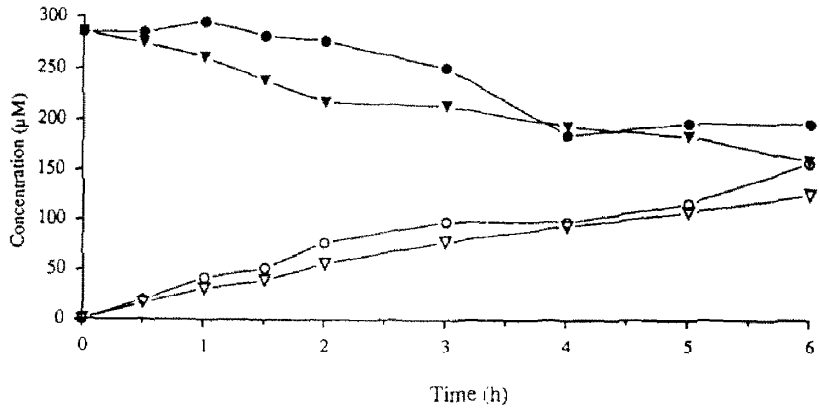

Fig. 5. Comparison of concentration profiles for the digestion of NEO by a *P. staminea* carbamoylase using CE–UV (triangles) and CE–ES-MS with selected ion monitoring (circles). NEO and dc-NEO are represented by filled and open symbols, respectively.

original NEO peak area was observed within the first 30 min of the reaction. Using both CE–UV and CE–ES-MS a decrease in NEO concentration of approximately 50% was detected after 6 h of incubation (Fig. 5), and more than 90% conversion was observed for incubation times longer than 15 h. The decrease in NEO concentration was paralleled by a concurrent increase of the dc-NEO peak area. In fact the sum of the two corrected areas observed in CE–UV experiments was found to be constant and equal to the original NEO peak area to within experimental uncertainties (± 8%). No other major components were observed on the corresponding CE–UV electropherograms. The CE–ES-MS analyses performed on the same fractions using selected ion monitoring (Fig. 5) were consistent with these observations, and showed excellent correlation with data obtained independently using CE–UV. Furthermore, CE–ES-MS analyses performed in full mass scan acquisition mode confirmed that the reaction product was indeed dc-NEO, and that no other major products were detected in the chosen mass range (m/z 200–500). Evidence accumulated thus far indicated that the decarbamoyl toxin is the only product released from the incubation with the crude clam extract. However, further studies were required to address this point as the enzyme specificity and affinity might vary depending on the type of substrate investigated.

Incubation of both N-sulfocarbamoyl and carbamoyl toxins in homogenates of *P. staminea* resulted in hydrolysis of the carbamate ester bonds of all PSP toxins. The rate at which this conversion took place was found to be highly dependent on the structure of the toxin. Previous studies [14] using HPLC–FLD indicated that formation of the decarbamoyl toxin was significantly faster for the N-sulfocarbamoyl toxins than for substrates such as STX, GTX_2 and GTX_3, although no measurements of activity were reported. A comparison of CE–ES-MS profiles obtained for different PSP toxins, following incubation periods of 15 h in all cases, is shown in Fig. 6. Each electropherogram represents the RIE profile corresponding to the MH^+ ions of the substrates and their corresponding decarbamoyl derivatives extracted from the full mass scan acquisition (m/z 200–500). The concentrations of the PSP toxins prior to the CE–ES-MS analysis were approximately 250 μM in all cases with the exception of GTX_3, C_1 and C_2 for which the concentrations were 60, 180 and 110 μM, respectively. An aliquot of 160 μl of the crude clam extract was added to each substrate solution.

Consistent with previous investigations [14], faster rates of enzymatic hydrolysis were observed for N-sulfocarbamoyl toxins such as B_1 (Fig. 6C) and $C_{1,2}$ (Fig. 6E) toxins. Amongst all toxins investigated, the formation of decarbamoyl toxin appears to proceed fastest for the sulfocarbamoyl toxin B_1, which was entirely converted to the dc-STX after 15 h of digestion (Fig. 6C). No signal was detected for B_1 which migrates at 25 min. under these conditions. In contrast, carbamate toxins such as STX (Fig. 6A) and NEO (Fig. 6B) displayed much slower reaction rates, and abundant MH^+ ions were observed for both the reaction products and the substrates after the same period of incubation.

Slower enzymatic activity was observed for the $GTX_{2,3}$ toxins (Fig. 6D) for which only a small fraction (typically less than 25%) was converted into the dc-$GTX_{2,3}$ toxins even after 15 h of incubation. In contrast, the formation of dc-$GTX_{2,3}$ toxins from the $C_{1,2}$ toxins (Fig. 6E) proceeded more rapidly, although the latter toxins differ from the $GTX_{2,3}$ toxins only by an extra sulfonate functionality at the N-21 position. It is noteworthy that the $GTX_{2,3}$ toxins observed in Fig. 6E correspond to residual impurities which were not totally separated from the C toxins during purification by column chromatography on Bio-Gel P-2. Interestingly, the hydrolysis of the $C_{1,2}$ toxins also gave rise to two additional peaks at 20.5 and 21.0 min. Abundant ions at m/z 353 were observed in the extracted mass spectra for these two components suggesting that these compounds could be isomers of dc-$GTX_{2,3}$. Fragment ions characteristic of dc-$GTX_{2,3}$, such as those corresponding to losses of H_2O and/or SO_3 (m/z 335, 273 and 255) were also observed for these two minor peaks in CE–ES-MS analyses conducted in selected ion moni-

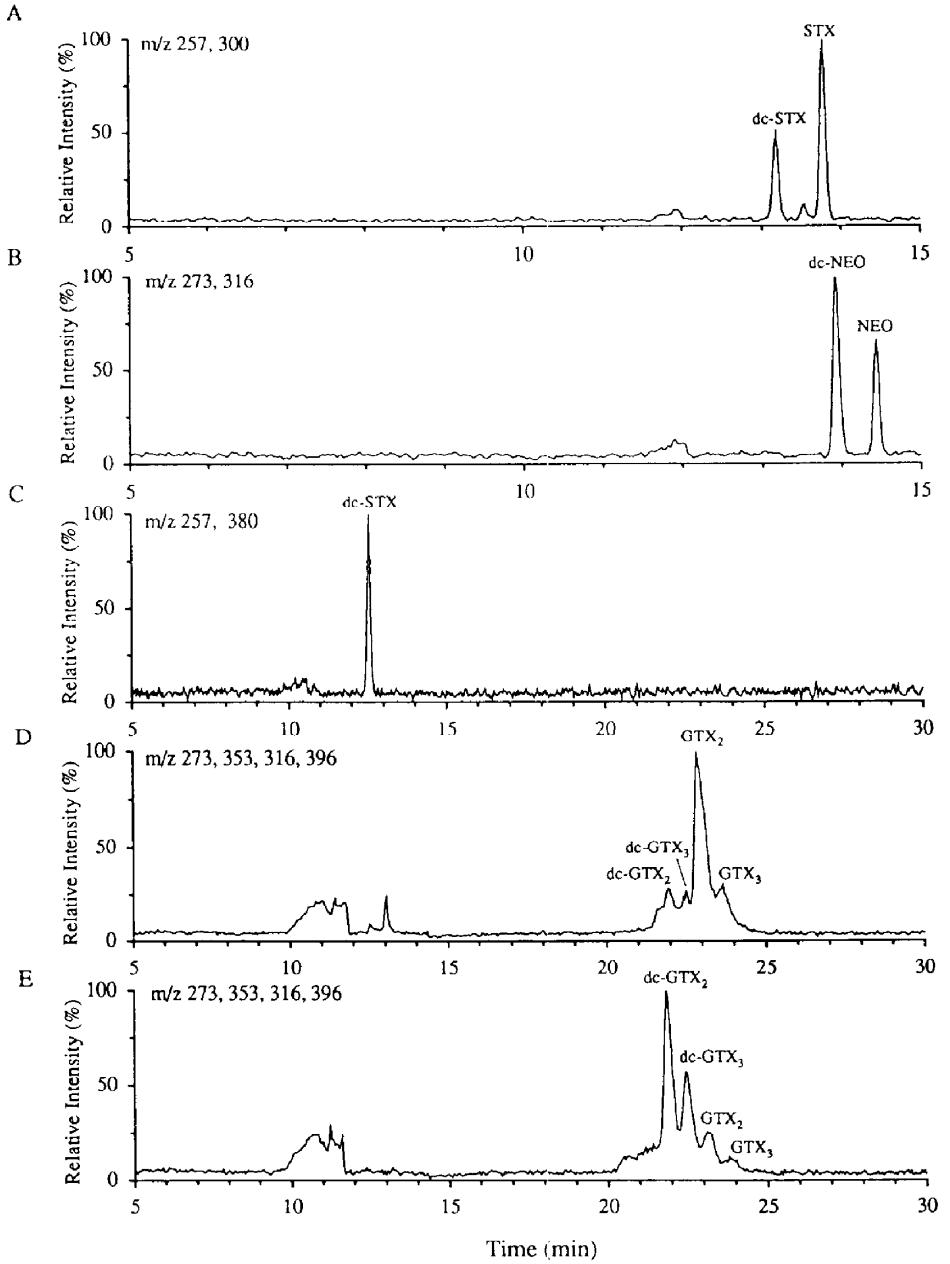

Fig. 6. CE–ES-MS analyses of different PSP standards following 15 h carbamoylase digestion. Reconstructed ion electropherograms for characteristic ions corresponding to substrates and decarbamoyl products of STX, 300 μM (A), NEO, 300 μM (B), B_1, 210 μM (C), GTX_2, 250 μM and GTX_3, 60 μM (D) and C_1, 180 μM and C_2, 110 μM (E). Conditions as in Fig. 3, concentrations given correspond to initial substrate concentrations.

toring mode (data not shown). However the exact structures of these dc-$GTX_{2,3}$ isomers are still not known at present. The occurrence of such dc-$GTX_{2,3}$ isomers was found only in digests of the C toxins, and could possibly arise from $C_{1,2}$ isomers present in the original substrate solution. Interestingly, a similar situation was encountered for STX where a small peak

was observed at 13.5 min in Fig. 6A. This component, which migrates just before STX, was also observed in CE–UV analyses of the STX standard solution, and accounted for approximately 3% of the STX peak area. The extracted mass spectrum of this minor component showed an abundant ion at m/z 300, suggesting that this compound could be an isomer of STX. Unfortunately, no previous report has documented such an observation, possibly reflecting the difficulties in obtaining sizable amounts of these two closely related PSP toxins using preparative chromatographic techniques.

The present CE stacking technique also facilitated the structural characterization of products released during the enzymatic hydrolysis using CE–ES-MS–MS. Examples of MS–MS spectra obtained are shown in Fig. 7A–D for MH^+ ions of dc-STX, dc-NEO, dc-GTX_2 and dc-GTX_3, respectively. In each case the extracted spectrum was obtained from the injection of 20 nl of the reaction mixture, and corresponded to the average of 3 to 4 scans across the CE peak. The MS–MS spectrum of the MH^+ ions of dc-STX (Fig. 7A) was characterized by sequential losses of H_2O and NH_3 giving rise to fragment ions at m/z 239 and 222. An abundant fragment ion at m/z 180, possibly arising from a rearrangement reaction favoring the elimination of a molecule of HN = C = NH from m/z 222, was also observed in Fig. 7A. Similar fragmentations were observed (Fig. 7B) in the MS–MS spectrum of MH^+ from dc-NEO with one additional fragment ion at m/z 225 possibly arising from the consecutive or concomitant losses of the C-17 side chain plus the hydroxyl group on N-1 (Fig. 1). Such a dissociation would lead to the formation of a conjugated double bond between N-1 and C-6, providing additional stability to the resulting fragment ion [19].

In comparison, the MS–MS spectra of MH^+ ions of dc-GTX_2 (Fig. 7C) and dc-GTX_3 (Fig. 7D), obtained from the enzymatic digestion of $C_{1,2}$ toxins, yielded much simpler fragmentation patterns than those of dc-STX or dc-NEO. The MS–MS spectra of these 11-sulfate derivatives were mostly dominated by losses of SO_3 and/or H_2O from the precursor ion. These two epimers, which only differ in the stereochemistry of the sulfate group on C-11 (Fig. 1), can be distinguished on the basis of the relative intensities of the fragment ions at m/z 255 and 273. For dc-GTX_3 the sulfate group is stabilized through interaction with the hydroxyl group on C-17, in a fashion similar to that described for $GTX_{2,3}$ [22], thus preventing the formation of the m/z 273 ion. Fragment ions observed in the MS–MS spectra of these decarbamoyl toxins formed as enzymatic hydrolysis products, were consistent with those of native PSP toxins [19,22], thus confirming the proposed assignments.

In order to determine the relative specificity and affinity of the crude preparation of the carbamoylase enzyme toward different substrates, the temporal profile of the digestion was monitored using CE–UV for a series of PSP toxins. Results obtained in these experiments are presented separately in Fig. 8 for the carbamate toxins (STX and NEO), the 11-sulfate carbamate toxins (GTX_{1-4}) and for the N-sulfocarbamate toxins (B_1 and $C_{1,2}$). The initial concentrations of PSP toxin substrates ranged from 70 to 440 μM while a constant aliquot of the concentrated enzyme extract was added to each of the toxin solutions. These initial substrate concentrations were not limiting, and comparisons of specificities for the different toxins are based on initial reaction rates only. Furthermore, it was not possible to use identical toxin concentrations to study these reactions because of the rapid formation of epimeric equilibria for solutions of the 11-sulfate analogues (as described later).

Amongst the three groups of toxins studied, the N-sulfocarbamate derivatives exhibited the fastest rate of hydrolysis. For example, incubation periods of approximately 0.5 and 3 h were required to convert 50% of the B_1 toxin and $C_{1,2}$ toxins into their corresponding decarbamoyl products, whereas more than 8 h was necessary to hydrolyse the same proportion of any of the other PSP toxins. This is evidenced in Fig. 8 from the slopes of the different digestion profiles. The formation of dc-STX from B_1 rapidly levelled off to its maximum value of approximately 200 μM after only 1.5 h. The production of dc-GTX_3 from the C_2 toxin followed a profile

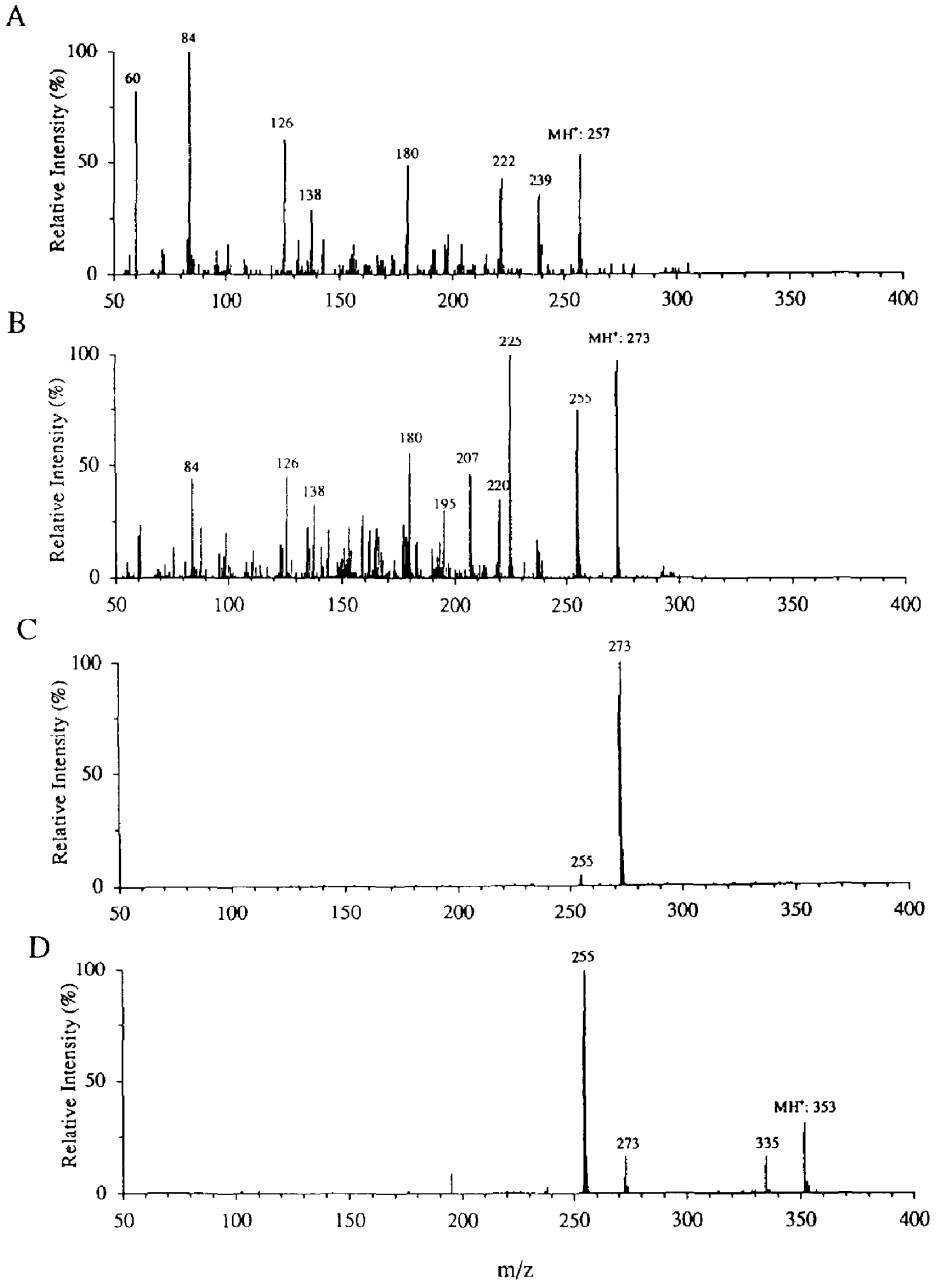

Fig. 7. CE–ES-MS–MS analyses of enzymatic products released during the carbamoylase digestion. Product ion mass spectra for dc-STX, *m/z* 257 (A), dc-NEO, *m/z* 273 (B), dc-GTX_2, *m/z* 353 (C) and dc-GTX_3, *m/z* 353 (D). Electrophoretic conditions as in Fig. 3, collision energies of 25 eV (laboratory-frame of reference) with Ar at collision gas thickness of $3.8 \cdot 10^{15}$ atoms cm^{-2}.

of hydrolysis similar to that of B_1 reaching a plateau after 1–2 h. The formation of dc-GTX_2 from C_1 appears to be more gradual reaching concentrations even higher than that of dc-GTX_3 after 6 h of incubation. The first-order rate constants were determined from the slopes of the

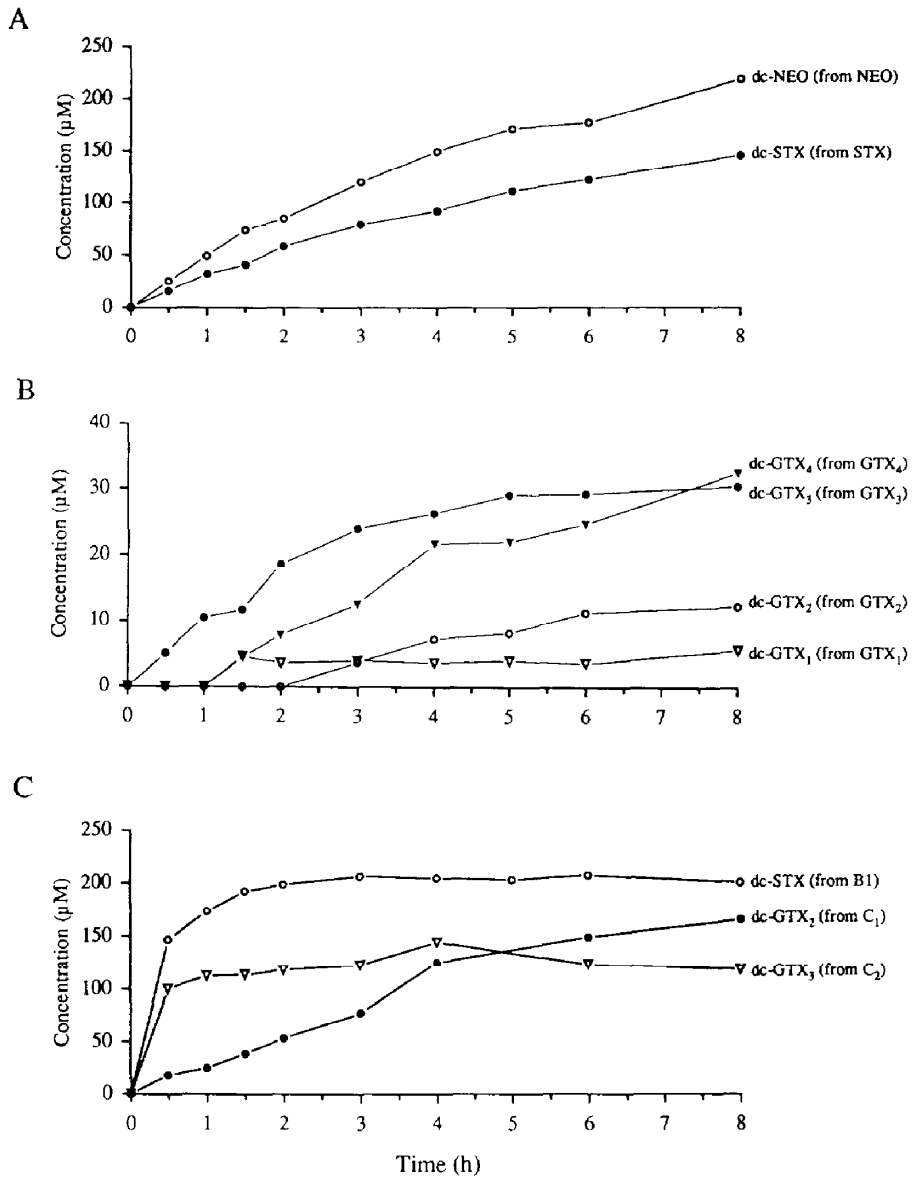

Fig. 8. Concentrations of decarbamoyl toxins released during the carbamoylase digestion of different PSP toxin substrates. Concentration profiles for carbamate toxins (A), 11-sulfocarbamoyl toxins (B) and N-sulfocarbamoyl toxins (C). Electrophoretic conditions as in Fig. 2, all concentrations were determined from CE–UV corrected peak areas. All toxin solutions were incubated with 140 μl of a crude clam homogenate extract. The initial substrate concentrations were as follows: STX (370 μM), NEO (440 μM), GTX_2 (120 μM), GTX_3 (90 μM), GTX_1 (310 μM), GTX_4 (70 μM), B_1 (210 μM), C_1 (180 μM), C_2 (110 μM).

natural logarithm of concentration vs. time for the first 2 h to be 1.1, 2.5 and 0.32 h^{-1} for B_1, C_2 and C_1, respectively.

The fact that the concentration of dc-GTX_2 overtakes that of dc-GTX_3 over a longer digestion period may reflect epimerization of the toxins in neutral buffers. The epimerization of substituents at the C-11 position follows a thermodynamic equilibrium with the α-epimer (C_1, C_3, GTX_1 and GTX_2) being more stable

than the β-epimer (C_2, C_4, GTX_3 and GTX_4) [4]. This trend was also noted in Fig. 8B, though to a much lesser extent, for dc-GTX_2 and dc-GTX_3 produced directly from the corresponding GTX_2 and GTX_3 toxins. In this latter case, the concentration of dc-GTX_3 declined after 5 h of incubation as a result of the epimerization of the C-11 sulfated derivatives. For the GTX toxins which are more resistant to decarbamoylation, the rate of individual toxin hydrolysis is complicated by epimerization reactions taking place at the same time.

The rate of hydrolysis of PSP toxins such as STX and NEO were found to be intermediate between the N-sulfocarbamoyl and the GTX toxins. For a given enzyme extract concentration, the natural logarithmic plots of STX and NEO concentrations vs. time gave good linearity with correlation coefficients $r^2 > 0.985$ over the 8-h incubation period. For these two toxins the plots of the natural logarithm of concentration vs. time showed an inverse linear relationship, consistent with a first-order reaction. The rate constants obtained from the slopes of these plots were $6.2 \cdot 10^{-2}$ and $8.3 \cdot 10^{-2}$ h^{-1} for STX and NEO, respectively, and indicated that 50% hydrolysis is reached at 11 and 8 h for the same two toxins. Unfortunately the rate constants for the GTX toxins could not be determined precisely from this preferred procedure using the integrated rate expression, since both the substrates and their enzymatic products are affected by epimerization reactions taking place under the present conditions. However, it is possible to evaluate approximately the relative reaction rates from the initial slopes of formation of dc-GTX toxins (Fig. 8B). Accordingly, the rate of GTX toxin hydrolysis increased progressively for GTX_2, GTX_1, GTX_3 and GTX_4. It is noteworthy that the concentration at which a plateau is observed appears to depends on the initial substrate concentration. Based on the above observations, the relative rate of hydrolytic conversion of PSP toxins into their corresponding decarbamoyl derivatives appears to observe the following progression: $C_2 > B_1 > C_1 > NEO > STX > GTX_4 > GTX_3 > GTX_1 > GTX_2$.

Although the relative susceptibilities of these toxins to hydrolysis is not a precise measure of their specific activities, the above progression is however indicative of the affinity of the enzyme for a given substrate. The fast hydrolysis rates noted for the N-sulfocarbamoyl toxins suggests the participation of the sulfo group in the enzymatic reaction. The presence of such a polar group near the hydrolysis site might facilitate the interaction of the substrate with basic residues of the catalytic site. Interestingly, hydrolysis rates were also found to be dependent on the orientation of the sulfate group on C-11, faster rates being observed for the β-epimers. While the configuration of the β-epimers would lead to more proximal interactions between the carbamoyl and 11-sulfate functional groups, it is possible that significant steric hindrance of the substrate as it approaches the catalytic site might be responsible for the lower hydrolytic activity of the carbamoylase for the 11α-sulfate toxins. Additional insights on the interactions of the substrate with the carbamoylase enzyme will possibly be obtained by comparison with similar hydrolytic enzymes, and through detailed structural analyses from X-ray diffraction studies. The development of isolation and purification procedures of the carbamoylase from *P. staminae* using the present screening method are presently in progress, and results from this latter study will be reported separately.

4. Conclusions

Improvements in sample focusing prior to zone electrophoresis separation were obtained for PSP toxins dissolved in high-ionic-strength buffers using on-column sample stacking. With proper choice of leading and terminating electrolytes, the method developed can be used with uncoated capillaries. The application of this stacking procedure is demonstrated for the analysis of products released during the digestion of PSP toxins by a carbamoylase isolated from viscera of little neck clams (*P. staminea*). This CE method was also used for detecting the desired enzymatic activity in fractions obtained from preparative chromatographic procedures. The ease of operation, flexibility, high resolution, and short analysis time of CE combined

with either UV or MS detection make this technique an attractive method for the monitoring of carbamoylase activity in shellfish extracts.

The identity of products formed during the enzymatic digestion of the PSP toxins was established directly by combined CE–ES-MS and CE–ES-MS–MS analyses. Results from this study provide direct evidence of the transformation of PSP toxins to decarbamoyl derivatives, and support a previous proposals made on the basis of indirect evidence from HPLC–FLD analyses of compounds obtained following re-carbamoylation of the enzymatic products [14]. The possibilities of conducting fast (less than 15 min) and reproducible analyses on crude clam extracts enabled determination of enzymatic profiles for different PSP toxin substrates. The rate of hydrolysis was also found to be highly dependent on the substrate structure. Amongst all PSP toxins investigated, the fastest rate of hydrolysis was found for the N-sulfocarbamoyl derivatives (B_1, C_1 and C_2) with rate constants ranging from 0.3 to 2.5 h^{-1}. In contrast, the formation of decarbamoyl products from any of the other PSP toxins proceeded more slowly with rate constants of less than $9 \cdot 10^{-2}$ h^{-1}. Furthermore, faster hydrolysis rates were observed for 11β-sulfate toxins such as C_2, GTX_3 and GTX_4 compared to their corresponding α-epimers (C_1, GTX_1 and GTX_2). This presumably reflects the steric hindrance of the substrate approaching the catalytic site.

Acknowledgements

The authors would like to thank R. Richards for technical assistance in preparing several of the PSP standards used in the present study, and Dr. A.D. Cembella and Dr. R.K. Boyd for valuable discussions.

Note added in proof

Additional experiments using CE–UV and CE–ES–MS enabled identification of neosaxitoxinol as the minor component observed at 13.5 min in Fig. 6A. Neosaxitoxinol is a C_{12} dehydroxy derivative of NEO, and can be obtained from reduction of NEO using sodium borohydride.

References

[1] S. Hall, P.B. Reichardt, in E.P. Ragelis (Editor), *Seafood Toxins (ACS Symposium Series*, No. 262), American Chemical Society, Washington, DC, 1984, p. 113.
[2] Y. Shimizu, in A.T. Tu (Editor), *Handbook of Natural Toxins, Vol. 3, Marine Toxins and Venoms*, Marcel Dekker, New York, 1988, p. 63.
[3] A.D. Cembella, J.J. Sullivan, G.L. Boyer, F.J.R. Taylor, R.J. Andersen, *Biochem. System. Ecol.*, 15 (1989), 171.
[4] A.D. Cembella, S.E. Shumway and N.I. Lewis, *J. Shellfish Res.*, 12, (1993) 389.
[5] P. Lassus, J.M. Frémy, M. Ledoux, M. Bardouil and M. Bohec, *Toxicon*, 27 (1989) 1313.
[6] P. Lassus, M. Bardouil, M. Ledoux, I. Murail, M. Bohec, P. Truquet, J.-M. Frémy and V. Rohmer, *Aquat. Liv. Res.*, 5 (1992) 319.
[7] V.M. Bricelj, J.H. Lee, A.D. Cembella and D.M. Anderson, *Mar. Ecol. Prog. Ser.*, 63 (1990) 177.
[8] V.M. Bricelj, J.H. Lee and A.D. Cembella, *Mar. Ecol. Prog. Ser.*, 74 (1991) 33.
[9] M.K. Beitler and J. Liston, in E. Granéli, B. Sundström, L. Edler and D.M. Anderson (Editors), *Toxic Marine Phytoplankton*, Elsevier, New York, 1990, pp. 257–262.
[10] Y. Shimizu, W.E. Fallon, J.C. Wekell, D. Gerber and E.J. Gauglitz, *J. Agric. Food Chem.*, 26 (1978) 878.
[11] Y. Shimizu and M. Yoshioka, *Science*, 212 (1981) 547.
[12] Y. Kotaki, Y. Oshima and T. Yasumoto, in D.M. Anderson, A.W. White and D.G. Baden (Editors), *Toxic Dinoflagellates —Proc. 3rd Int. Conf. on Toxic Dinoflagellates*, Elsevier, New York, 1985, pp. 287–292.
[13] Y. Oshima, in P. Lassus (Editor), *Proceedings of the 6th International Conference on Toxic Phytoplankton, Nantes, 18–22 October 1993*, Elsevier, p. 153.
[14] J. Sullivan, W.T. Iwaoka and J. Liston, *Biochem. Biophys Res. Commun.*, 114 (1983) 465.
[15] J. Sullivan, M.M. Wekell and L.L. Kentala, *J. Food Sci.*, 50 (1985) 26.
[16] Y. Oshima, M. Machida, K. Sasaki, Y. Tamaoki and T. Yasumoto, *Agric. Biol. Chem.*, 48 (1984) 1707.
[17] P. Thibault, M.V. Laycock and S. Pleasance, *J. Chromatogr.*, 542 (1991) 483.
[18] S. Pleasance, P. Thibault and J.F. Kelly, *J. Chromatogr.*, 591 (1992) 325.
[19] S.J. Locke and P. Thibault, *Anal. Chem.*, 66 (1994) 3436.
[20] M.V. Laycock, P. Thibault, S.W. Ayer and J.A. Walter, *Natural Toxins*, 2 (1994) 175.
[21] R.D. Smith, J.A. Olivares, N. Nguyen and H.R. Udseth, *Anal. Chem.*, 60 (1988) 436.
[22] S. Pleasance, S.W. Ayer, M.V. Laycock and P. Thibault, *Rapid Commun. Mass Spectrom.*, 6 (1992) 14.